NF_3/CH_4 플라즈마를 이용한 실리콘 카바이드 식각공정의 신경망 모델링

김병환, 이석룡*, 이병택*, 권광호**
세종대학교 전자공학과, 전남대학교 재료과학공학과*, 한서대학교 전자공학과**

Modeling of silicon carbide etching in a NF_3/CH_4 plasma using neural network

Kim Byungwhan, Lee Suk Yong*, Lee Byung Teak*, Kwon Kwangho**
Sejong Univ., Chonnam National Univ.*, Hanseo Univ.**

Abstract

Silicon carbide (SiC) was etched in a NF_3/CH_4 inductively coupled plasma. The etch process was modeled by using a neural network called generalized regression neural network (GRNN). For modeling, the process was characterized by a 2^4 full factorial experiment with one center point. To test model appropriateness, additional test data of 16 experiments were conducted. Particularly, the GRNN predictive capability was drastically improved by a genetic algorithm (GA). This was demonstrated by an improvement of more than 80% compared to a conventionally obtained model. Predicted model behaviors were highly consistent with actual measurements. From the optimized model, several plots were generated to examine etch rate variation under various plasma conditions. Unlike the typical behavior, the etch rate variation was quite different depending on the bias power. Under lower bias powers, the source power effect was strongly dependent on induced dc bias. The etch rate was strongly correated to the dc bias induced by the gas ratio. Particularly, the etch rate variation with the bias power at different gas ratio seemed to be limited by the etchant supply.

Key Words : Plasma etching, model, neural network, genetic algorithm

1. Introduction

Silicon carbide (SiC) has been widely used to fabricate high power, high temperature devices. Due to high bond energy between silicon and carbon, plasma-assisted etching has been used to pattern the SiC [1-14]. Desired features in SiC *etching include high etch rate, high* anisotropy with no trench, and smooth surface with no residues. Although capacitively coupled reactive ion etching is effective to bond-breaking due to high ion energy, it may cause mask erosion and residual surface lattice damage. To circumvent this, inductively coupled plasma (ICP) has been used in SiC etching. Apart from high plasma density, the ICP provides lower ion energy and the capability to operate at lower chamber pressures. Moreover, ion fluxes and ion energy can be separately controlled, thus increasing flexibility in optimizing etch responses. To optimize SiC etch process in a cost effective way, a predictive model is highly demanded. The model can effectively be used to identify some trade-offs between etch responses as a function of process parameters. For this, a neural network approach combined with a statistical experimental design has been used to characterize relationships

between the process parameters and etch responses during the SiC etching in a C_2F_6 ICP [3-5].

In this study, SiC films are etched in a NF_3/CH_4 ICP. The process was characterized by a statistical experimental design. Process parameters that were experimentally varied include radio frequency (rf) source power, bias power, pressure, and NF_3 percentage. A predictive model of the etch rate is constructed by using a neural network called generalized regression neural network (GRNN) [15]. The GRNN prediction accuracy is optimized by means of a genetic algorithm (GA) [16]. From the optimized model, the etch rate is qualitatively interpreted as a function of process parameters. The dc bias is also correlated to a variation in the etch rate.

Table 1. Parameters and experimetnal ranges

Parameters	Ranges	Units
Source Power	700-900	Watts
Bias Power	50-150	Watts
Pressure	6-12	mTorr
Gas Ratio	0.2-1.0	%

2. Experimental Details

The schematic of an etch sustem has already been presented in our previous studie [3,4,5]. Test patterns were fabricated on n-type, 2 inch 4H-SiC wafers of <0001> orientation. To fabricate a Ni mask layer, photo resist (PR) patterns were first formed using a Cr negative mask. Using a magnetron sputter, a Ni layer was then deposited by about 0.15㎛. By removing PR patterns using the lift-off process, the Ni mask was finally obtained. The SiC films were etched in a NF_3/CH_4 plasma. In all experiments, the etching was conducted for the same 5 minutes. The process parameters examined include the rf source power, bias power, pressure, and NF_3 percentage. The percentage is defined as a ratio of the NF_3 flow rate to the total flow rate, i.e., the sum of NF_3 and CH_4 flow rates. The total flow rate was set to 30 sccm in every experiment. The etch rate was estimated by using a scanning electron microscopy (SEM). The dc self-bias was measured and correlated to the etch rate.

The etch process was characterized by a 2^4 full factorial experiment. The parameters and experimental ranges are contained in Table 1.

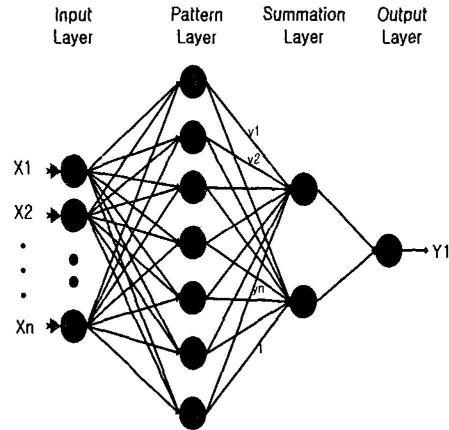

Fig 1. Schematic of GRNN architecture.

3. GA-optimized Neural Network

A schematic of GRNN structure is depicted in Fig. 1. Each neuron in the pattern layer is equipped with a Gaussian D function defined as

$$D(x, x_i) = \sum_{j=1}^{p} \left(\frac{x_j - x_{ij}}{\zeta}\right)^2$$

where p indicates the number of elecments of an input vector. The x_j and x_{ij} represent jth element of x and x_i, repsectively. ζ is called "spread" and determines the GRNN prediction performance. Once optimized, in most applications, all neurons have the same spread. This critically limits the GRNN predictive ability. To overcome this, GA is used to control the spreads. In GA optimization, the spreads for all neurons in the pattern layer were ranged between 0 and 0.4. The initial population was set to 200 potential solutions. The probabilities of crossover and mutation were set to 0.9 and 0.01, respectively. The search process was terminated as the generation number reaches its predefined value of 100. The finally determined

model has the RMSE of 7.0 nm/min. Compared to the conventional model, this demonstrates an improvement of about 83.2%. In consequence, the GA dramatically improved the GRNN prediction accuracy.

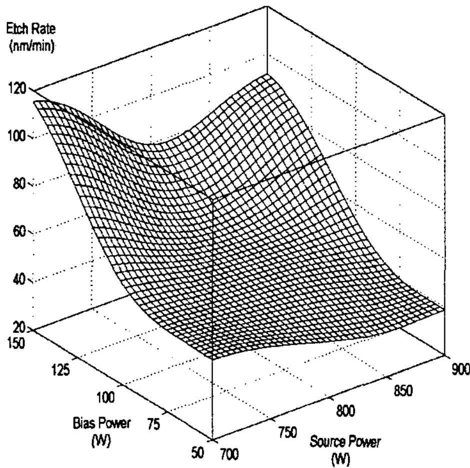

Fig 2. Etch rate as a function of source and bias powers.

4. Conclusion

4.1 RF source and bias powers

From the optimized model, plots were generated to examine parameter effects on the etch rate. Figure 2 shows an etch rate as a function of bias and source powers. The other pressure and gas ratio was set to 9 mTorr and 0.6, respectively. As depicted in Fig. 2, the etch rate increases considerably by increasing the bias power (i.e., *ion bombardment*). This indicates that the etch rate is determined predominantly by the bias power. This behavior is supported by the experiments conducted at 800 W source power. Actually, the etch rate increased from 40 nm/min to 80 nm/min with increasing the bias power from 50 W to 150 W. Larger etch rate at higher bias power is typically ascribed to enhanced ion bombardment. Meanwhile, the increase in the etch rate is observed over the entire range of the source power. This clearly demonstrates that in current high density plasma etcher available both plasma density and ion bombardment energy is separately controlled.

As depicted in Fig. 2, the etch rate initially decreases and then increases with increasing the source power at higher bias powers more than about 100 W. This etch rate behavior is completely different from the typical one, i.e., a continuous increase in the etch rate with an increase in the source power [6,7]. To verify this particular model trend, etch experiments were conducted at 100 W bias power with the other parameters set to the same plasma conditions as those employed in Fig. 2. The experiments reveal that the etch rate decreased from 58 *nm/min to* 56 *nm/min with increasing* the source power from 700 W to 800 W. When the source power increased to 900 W, in contrast, the etch rate increased to 60 nm/min. Therefore, the complex etch rate behavior observed was *experimentally* certified. The verified consistency supports that the constructed etch rate model is highly accurate. From the complex behavior, meanwhile, the etch rate is expected dominated by two different etch mechanisms depending on the level of the source power. Physical phenomena typically accompanied with a variation in the source power in the combined NF_3 and CH_4 discharge are variation in the dc bias or plasma density. When increasing the source from 700 W to 800 W, The dc bias decreased from 390 V to 377 V. Thus, the initially decreased etch rate is strongly correlated to the reduced dc bias. This is supported from the strong dependency of the etch rate on the bias power as observed earlier. Another expected effect is an increase in F concentration [F] by an increase in plasma density. By the strong correlation between the etch rate and dc bias, however, it is expected that for the source powers between 700 and 800 W the ion bombardment effect prevails over the etchant-driven one. Meanwhile, the dc bias varied by only 1 V for the variation in the source power from 800 W to 900 W. This represents the insignificant impact of the dc bias. By considering this effect, the increased

etch rate observed in this source power range can mainly be attributed to increased F density. In consequence, the crossover point in the etch rate was caused by the competing effects between the dc bias and etchant supply. As displayed in Fig. 2, the complex trend becomes more conspicuous at higher bias power while being substantially weakened at lower ones. The etch rate seems to even decrease with increasing the source power at 50 W. This unexpected behavior is partly supported by the experiments conducted at the same 50 W bias power, but at 12 mTorr pressure and 0.2 gas ratio. Under this plasma condition, the etch rate decreased from 30 nm/min to 19 nm/min with increasing the source power 700 W to 900 W, respectively. The corresponding dc bias varied only by 1 V. Thus, the little varied etch rate is closely related to the dc bias. From these observations, the etch rate seems to be dominated by the source power-induced dc bias at lower bias powers. Under high bias powers, the etch rate was strongly dependent on the dc bias in the low source power range. In the high source power range, it was dominated by variations in plasma density, i.e., the supply of F etchant.

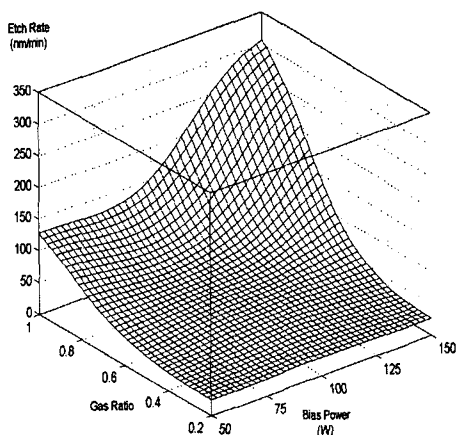

Fig 3. Etch rate as a function of bias power and gas ratio.

4.2 RF bias power and gas ratio

Figure 3 shows a variation in the etch rate with the bias power and gas ratio. The other source power and pressure were set to 800 W and 9 mTorr, respectively. As depicted in Fig. 3, the etch rate increases with increasing the gas ratio at 100 W bias power. Larger increase in the etch rate at higher gas ratio is represented on the corresponding response surface. To certify this, etch experiments were conducted at the same 100 W. The experiments reveal that the etch rate increased from 22 nm/min to 56 nm/min by about 34 nm/min with increasing the gas ratio from 0.2 to 0.6. At the highest gas ratio 1.0, the etch rate increased to 154 nm/min. With respect to the etch rate at the medium gas ratio 0.6, the variation is about 98 nm/min. As a result, the etch rate variation with the gas ratio is experimentally verified. Similarly as observed in earlier, the etch rate is strongly related to a variation in the dc bias since it increased from 312 V to 409 V with increasing the gas ratio from 0.2 to 1.0, respectively. Meanwhile, the [F] is expected to increase with increasing the gas ratio. Therefore, its contribution to the increase in the etch rate needs to be taken into account. In this sense, the increased etch rate can be attributed to the combined effect of increased dc bias and F density. The increase is more conspicuous at higher bias powers, presumably due to the increased dc bias maintained within the chamber.

As displayed in Fig. 3, the bias power effect is complex depending on the gas ratio. The etch rate varies very little with increasing the bias power at the gas ratio 0.2. This behavior is completely different from the one observed as the bias power varied at different source powers as depicted in Fig. 2. In previous plasma etchings, this particular phenomenon has rarely been predicted or experimentally observed. This indicates the presence of strong interactions between the bias power and gas ratio. The etch rate behavior observed is partly supported by the experiments conducted at the gas ratio 0.2, but at 900 W source power and 12 mTorr

pressure. Here, the etch rate increased from 19 nm/min to 20 nm/min only by 1 nm/min. In contrast, the corresponding dc bias increased from 267 V to 450 V by 183 V. It is therefore clear that the dc bias is unable to be correlated to the etch rate variation. Rather than this, the etch rate remaining almost constant can mainly be ascribed to the chamber condition, where the etchant was not sufficiently supplied. This is more ascertained by the increasing etch rate at higher gas ratio as displayed in Fig. 3. In this condition, the etchant is expected sufficiently provided. In this sense, the etch rate variation with the bias power under various gas ratio is dominated by the etchant supply. This feature has rarely been charterized in previous etchings.

Acknowledgements

This work was supported by the Korean Ministry of Science and Technology through the National Research Laboratory Project.

References

[1] M. Kothandaraman, D. Alok, and B. J. Baliga, *J. Elect. Mat.* 25, 875 (1996).

[2] J. J. Wang, E. S. Lambers, S. J. Pearton, M. Ostling, C. M. Zetterling, J. M. Grow, and R. J. Shul, *J. Vac. Sci. Technol. A* 16, 2204 (1998).

[3] B. Kim and B. T. Lee, Plasma Chem. Plasma Proc. 23, 487 (2003).

[4] B. Kim, S. Kong, and B. T. Lee, J. Vac. Sci. Technol. A 20, 146 (2002).

[5] B. Kim, H. J. Choi, and B. T. Lee, J. Vac. Sci. Technol. A 20, 424 (2002).

[6] F. A. Khan and I. Adesida, *Appl. Phys. Lett.* 75, 2268 (1999).

[7] L. Cao, B. Li, and J. Zhao, *J. Electrochem. Soc.* 145, 3609 (1998).

[8] P. Chabert, G. Cunge, J. P. Booth, and J. Perrin, *Appl. Phys. Lett.* 79, 916 (2001).

[9] J. D. Scofield, B. N. Ganguly, and P. Bletzinger, *J. Vac. Sci. Technol. A* 18, 2175 (2000).

[10] S. K. Lee, S. M. Koo, C. M. Zetterling, and M. Ostling, *J. Elect. Mat.* 31, 340 (2002).

[11] P. H. Yih and A. J. Steckl, *J. Electrochem. Soc.* 142, 312 (1995).

[12] J. B. Casady, S. S. Mani, R. R. Siergiej, W. Urban, V. Balakrishna, P. A. Sanger, and C. D. Brandt, *J. Electrochem. Soc.* 145, L58 (1998).

[13] J. R. Flemish and K. Xie, *J. Electrochem. Soc.* 143, 2620 (1996).

[14] M. Syvajarvi, R. Yakimova, and E. Janzen, *J. Electrochem. Soc.* 147, 3519 (2000).

[15] D. F. Specht, *IEEE Trans. Neural Network* 2, 568 (1991).

[16] D. E. Goldbeg, *Genetic Algorithms in Search, Optimization & Machine Learning*, Addison Wesley, 1989.